ON THE BROAD BAND ENERGY DISTRIBUTION OF BLAZARS

Laura Maraschi
Dipartimento di Fisica, Università di Milano, via Celoria 16, 20133 Milano, Italy

Gabriele Ghisellini
Osservatorio di Torino, Strada Osservatorio 20, 10025 Torino, Italy

and

Annalisa Celotti
Institute of Astronomy, Madingley Road, Cambridge CB3 0HA, United Kingdom

Abstract. The broad band energy distributions of blazars are revisited with particular emphasis on the sources detected in γ–rays by the Compton Observatory (GRO). The observed distributions can be broken down into two main components, corresponding to two broad peaks in the νF_ν representation. The first occurs in the FIR–optical range, the second in the MeV–GeV region. In the case of MKN 421, which may be representative of X–ray selected BL Lacs, the first peak is shifted to higher frequency ($\simeq 10^{16}$ Hz) and the γ–ray spectrum extends to TeV energies. There is general agreement that the first spectral component is due to synchrotron radiation from a relativistic jet, although some problems remain in deriving the spectrum and location of the emitting relativistic electrons. The second component, which in most objects extends from the X–ray to the γ–ray range, can be naturally interpreted as inverse Compton scattering by the same electrons producing the synchrotron photons, either on the synchrotron photons themselves (SSC) or on photons external to the jet. It is argued that multifrequency studies of these sources including γ–rays will allow to test Inverse Compton models and to distinguish between different sources of photons.

Key words: Active Galactic Nuclei: blazars - Radiation Mechanisms: Synchrotron, Inverse Compton - UV - X–rays - γ–rays

1 Introduction

A blazar usually exhibits a compact radio core with flat or inverted spectrum, rapid variability at all wavelengths and significant optical polarization. There are two main subgroups within blazars: objects characterized by the absence or weakness of emission lines (EW$\leq$ 5 Å) are called BL Lacs while objects exhibiting typical quasar lines are designated as flat spectrum (FSQ) or core dominated (CDQ) or optically violently variable (OVV) or highly polarized (HPQ) quasars depending on which of the above properties is present and/or needs to be emphasized.

Of all Active Galactic Nuclei, blazars have the widest electromagnetic spectrum, extending from the radio to the γ–ray range. There is presently general agreement that the blazar continuum is due to non–thermal radiation emitted by plasma moving at relativistic speed (relativistic jet) in a direction close to the line of sight, as originally proposed by Blandford & Rees (1978). Synchrotron radiation can account for the emission up to the UV and, in some cases, X–ray band. Several models attribute the γ–ray emission to Inverse Compton scattering of relativistic electrons off various sources of soft photons (see e.g. Sikora 1993), but alternative

T. J.-L. Courvoisier and A. Blecha: Multi-Wavelength Continuum Emission of AGN, 221–232.

mechanisms have also been proposed (see e.g. Mannheim 1993, Ghisellini 1993)

A critical parameter in estimating the physical conditions in these objects is the Doppler or beaming factor $\delta = (\Gamma - \sqrt{\Gamma^2 - 1}\cos\theta)^{-1}$, where Γ is the bulk Lorentz factor and θ is the angle between the velocity and the line of sight. The observed power is related to that emitted in the rest frame of the jet by $L_{obs} = L_{int}\delta^p$, where $p = 4$ for a moving blob and $p = 3$ for a continuous jet of plasma.

Blazars as a class are characterized by bulk Lorentz factors of order 10, as directly shown by the superluminal knots and derived by a simple application of the SSC theory to the radio core (see Ghisellini et al. 1993). It is interesting to recall that the very condition of transparency to γ–rays, together with the short time scale variability, also allows to derive a lower limit to the beaming factor (Maraschi, Ghisellini & Celotti, 1992).

On average BL Lacs have similar Lorentz factors as CDQs, but lower beaming factors, implying somewhat larger average viewing angles (Madau et al. 1987, Ghisellini et al. 1993). Thus the idea that BL Lacs have emission lines comparable to those of CDQs, which are invisible because of a highly enhanced continuum, can be dismissed. We then conclude that the "thermal" power (including emission lines and the UV bump) in BL Lacs is intrinsically weak. Exceptions are possible, and some 'hidden' CDQs may be present among high redshift BL Lacs.

Here we summarize recent observational results on the broad band energy distributions of BL Lacs and CDQs, most notably the discovery of γ–ray emission, but also observations in the IR–optical–UV and X–ray bands, which improve our knowledge of the overall continuum shape (§2). In §3 we discuss synchrotron models for the continuum up to the UV and in some cases X–ray band. An interesting constraint (§4) is imposed by the observed correlation and delay of few hours between the UV and X–ray light curves of the BL Lac object PKS 2155–304. This object, together with MKN 421 and other X–ray bright BL Lacs may represent a subclass of BL Lacs with extreme values of the X–ray to radio flux ratio.

In §5 we discuss inverse Compton models for the production of γ–rays, where the scattering electrons are the same that produce the synchrotron continuum in the jet and the scattered photons may be either the synchrotron photons within the jet or ambient photons produced by other mechanisms outside the jet. We examine possible ways of discriminating between different models by studying the correlation of variability of γ–rays with other frequency bands.

2 Observed Energy Distributions

Systematic studies of the Broad Band Energy Distributions (BBED) of blazars were started by Impey and Neugebauer (1988) and followed by Ghisellini et al. (1986) and Landau et al. (1986). These authors found that the spectra from the radio to the UV band were "curved" in the sense that the "average slope" increased with frequency.

However, recent accurate simultaneous measurements in the IR–optical–UV

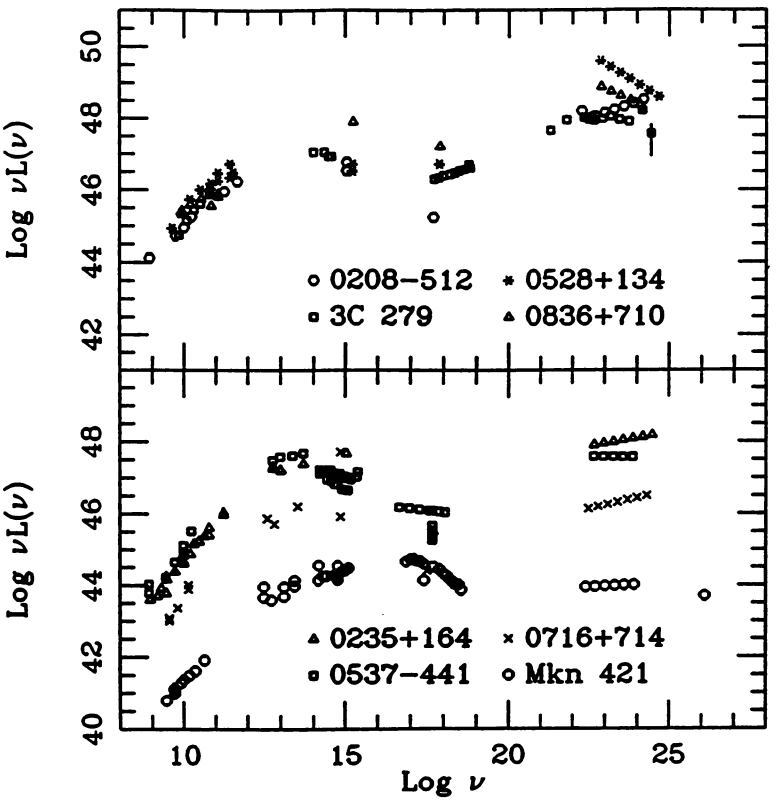

Fig. 1. The broad band energy distributions of 4 HPQs (upper panel) and 4 BL Lacs (lower panel) are plotted using the $\nu L(\nu)$ representation. The data are collected from the literature, and in general are not simultaneous. For 3C 279 see Hartmann et al. (1992) and Maraschi et al. (1992) and references therein; for PKS 0208–512 see Bertsch et al. (1993). For the other sources, radio data are from Kuhr et al. (1981), Wiren et al. (1992), Wall & Peacock (1985), Ledden & O'Dell (1985), Valtoja et al. (1992); far IR data from Impey & Neugebauer (1988); IR, optical and UV data from Maraschi et al. (1986), Ghisellini et al. (1986) and references therein, Tanzi et al. (1989), Kuhr et al. (1981); X–ray data from Worral & Wilkes (1990), Treves et al. (1993); γ–ray data from Hunter et al. (1993 a,b) Thompson et al. (1993 a,b) Lin et al. (1992), Punch et al. (1992).

bands (e.g. Falomo et al., Edelson, these proceedings) show that the continua of several objects are well described by a single power law in this extended range, contrary to the notion of continuous curvature. Giommi et al. (these proceedings), using archival data on BL Lacs, show that the BBED from the mm to the X–ray band can be described by two power laws with a break. Different objects are

https://doi.org/10.1017/S0074180900175072 Published online by Cambridge University Press

characterized mainly by a different break energy, while the spectral shape below and above the break is similar for all objects. Thus a new picture seems to emerge in which in individual objects changes of slope occur in relatively narrow frequency ranges. This is not inconsistent with the earlier results, if the increasing slope in the "average" spectrum is due to an increasing fraction of objects in the sample having break energy below the considered band.

Ghisellini at al. (1986) noted that the optical–UV continuum of X–ray selected BL Lacs was flatter than that of radio selected ones. This has been recently confirmed on a larger sample (25 radio selected, 8 X–ray selected) by Pian and Treves (1993). Adopting the above point of view, the flatter spectra may be due to a spectral break in X–ray selected objects occuring at a very high frequency.

The BBED up to the γ–ray range of 4 HPQs and 4 BL Lac objects are shown in Fig. 1. The chosen objects represent all BL Lacs, and representative cases among the 11 CDQs, for which the γ–ray flux and α_γ were available (Hartman et al. 1993). The BBED of the remaining 7 CDQs closely resemble those plotted in Fig. 1.

We note some remarkable features: the BBED of all objects show a relative maximum between the radio and X–ray bands. For HPQs the maximum should fall between the mm and IR bands (10^{12-14} Hz), a spectral region where only for few objects IRAS data are available.

For three of the BL Lacs the maximum falls in the same frequency interval as for HPQs (note that all the four BL Lacs have IRAS data.) However for MKN 421 the maximum occurs at a much higher frequency, close to 10^{16} Hz. In this case the X–ray spectrum is very steep and appears to be an extension of the optical–UV continuum. This seems to be a general property of the X–ray emission of radio weak, X–ray selected BL Lacs, which have an average spectral index of $< \alpha_X >= 1.4 \pm 0.1$ (Sambruna et al. 1993). Here and in the following α is always defined as $F_\nu \propto \nu^{-\alpha}$. On the contrary the X–ray spectra of HPQs are generally flat with $< \alpha_X > \sim 0.5$ while those of radio–strong BL Lacs appear intermediate, with $< \alpha_X > \sim 1$ (Worral & Wilkes, 1990)

Joining the X–ray flux with the γ–ray flux, a rising slope [in $\nu F(\nu)$] is obtained in all cases except for MKN 421. This indicates a new spectral component which we attribute to the inverse Compton process. For the four BL Lacs $\alpha_\gamma \leq 1$ indicating that the maximum power of this component is in or beyond the GeV range. In the case of MKN 421 the γ–ray emission extends up to TeV energies.

Of the 15 quasars with known α_γ, 10 have $\alpha_\gamma \geq 1$, indicating that the maximum power is emitted in or below the GeV range. The four cases reported in Fig. 1 have been chosen so as to include a flat and a steep case.

Another indication from Fig. 1 is that the ratio between the γ–ray luminosity and the maximum luminosity in the 10^9–10^{17} Hz range tends to be ≥ 1 for quasars, while it is ≤ 1 for BL Lacs. However, since for most objects the measurements in other bands are not simultaneous with the γ–ray observations and the objects are extremely variable, the ratio L_γ / L_{IROUVX} is at present highly uncertain.

In summary the BBED of blazars from radio to γ–ray frequencies may be de-

scribed as two smooth components: the first extends from 10^9 to 10^{17} Hz, with a broad maximum in the power per decade between 10^{12} and 10^{14} Hz for CDQs and radio selected BL Lacs, and at 10^{15-16} Hz for X–ray selected BL Lacs. The second extends from 10^{17} to 10^{25} Hz, peaking often in the 10^{22-24} Hz range but sometimes even beyond. The first will be called here the synchrotron component, the second will be called the inverse Compton component. Some theoretical problems relevant in the two domains are discussed below.

It is worth stressing that the present body of data on the BBED of blazars, though impressive, is still very incomplete. In particular simultaneous measurements in different frequency bands are needed.

3 The synchrotron component

The success of models explaining the evolution of radio flares, the significant polarization often observed in the optical and the spectral "continuity" leave little doubt that the emission mechanism from the radio to the UV is synchrotron radiation. It is also clear that the flat spectra observed in the radio ($\alpha_R \simeq 0$) are due to the superposition of synchrotron self–absorption turnovers of different emission regions (i.e. the jet is inhomogeneous), higher frequencies corresponding to more compact regions. Early models attempted a continuous "fluid" description of the inner jet to reproduce the overall radio to X–ray spectrum (e.g. Königl 1989), but models involving one or more discrete emission regions, probably associated with shocks, are also viable (e.g. Marscher 1993).

Above about 10^{12} Hz the emission becomes transparent and the spectrum steepens to $\alpha_{IR} \simeq 1$. Since only few objects have been detected with IRAS, the initial slope of the transparent synchrotron spectrum is poorly known. At higher frequencies, usually in the optical–UV band or in the X–ray band for the X–ray selected BL Lacs, the spectrum steepens to $\alpha \geq 1$, perhaps through a localized change in slope (break), rather than in the continuous fashion previously believed.

A steepening in the spectrum of non thermal electrons can be interpreted as due to radiation losses. In the case of continuous injection the break occurs at the energy for which the radiative life time equals the escape time of the particles from the emission region. Assuming the minimum escape time R/c and energy losses due to only the local energy density of radiation, it can be easily shown that the break occurs at $\gamma_b \sim 1/\ell$ where ℓ is the compactness parameter defined by $\ell = \sigma_T L/(R m_e c^3)$. This compactness refers to the frame of the emitting plasma, and is related to the observed quantities through $\ell = \ell_{obs}/\delta^{p+1}$, if R is derived from an observed variability time scale, $R = c t_{obs} \delta$. Sources with $\delta = 10$, $L_{obs} = 10^{46}$ erg/s and $t_{obs} = 1$ day should have $\ell = 10^{-3}$ (for $p = 4$), and therefore $\gamma_b \sim 10^3$. This corresponds to a synchrotron break frequency $\nu_b \sim 3 \times 10^{13} B$ Hz (where B is the magnetic field).

An alternative explored by Ghisellini, Maraschi & Treves (1985, hereinafter GMT) and Ghisellini & Maraschi (1989) is to interpret the steepening as a convo-

https://doi.org/10.1017/S0074180900175072 Published online by Cambridge University Press

lution of high energy cut–offs in emission regions of decreasing size with increasing energy. This choice was motivated by the short ($\simeq$ hours) timescales observed in the X–ray band. In this model the radiative loss timescales can be much shorter than R/c, which does not need to be the same at all frequencies.

More realistically, one or more shocks may be present in the inner regions of the jet. At the shock front particles should be accelerated and diffuse downstream, those of higher energy filling a smaller volume due to the shorter life time (see Bregman 1985). This case is intermediate between the two above, in that at all energies above the break the particle life time and the size of the emitting region are related. Bregman (1985) obtained an almost exponential steepening (larger than observed), but a more realistic treatment of particle acceleration and diffusion may yield better agreement with the present data.

4 The case of PKS 2155–304

Intensive multiwavelength observations of PKS 2155–304 have provided two major results: 1) the variability in the optical–UV and in X–rays is highly correlated on timescales of hours; 2) the UV light curve is delayed by $\simeq$ 3 hours with respect to X–rays, as measured in the ROSAT band (see Edelson these proceedings). The simultaneous overall spectrum of PKS 2155–304 obtained from these observations is shown in Fig. 2. The γ–ray upper limit is derived converting the limiting sensitivity of EGRET of 10^{-7} ph/(cm^2 sec) above 100 MeV.

These results show unambiguously that the X–ray and UV emitting regions are not coincident, in agreement with the GMT model. However the measured lag is small compared to the size of the UV emitting region, if the latter is related to the observed month long doubling timescale. Unfortunately the X–ray observations spanned only a four day period, due to the wisdom of allocation committees, and we have no information concerning the correlation of X–rays with the larger amplitude UV variation. Considering UV and X–ray observations in the higher GINGA band (Sembay et al. 1993), the correlation appears less tight, but no delay can be determined due to the sparse sampling.

In the context of emission from relativistic jets, studies of the variability behaviour of the high frequency emission have been carried out by Celotti, Maraschi & Treves (1991) and Marscher, Gear & Travis (1992).

The former consider a perturbation (shock) moving through an otherwise stationary jet, described by the model of GMT, causing the emission from different regions to vary at different times. Emission below the break frequency, i.e. in the IR–optical–UV bands, is produced in the same volume (see §3). Therefore it is expected to vary simultaneously, without spectral changes, if the perturbation affects the particle density but not their spectrum. Emission above the break (X–rays in the case of PKS 2155–304) derives from a smaller region, closer to the nucleus. Therefore it is affected first by a perturbation moving outward. The typical cooling time of the high energy electrons in the latter region can be shorter than the

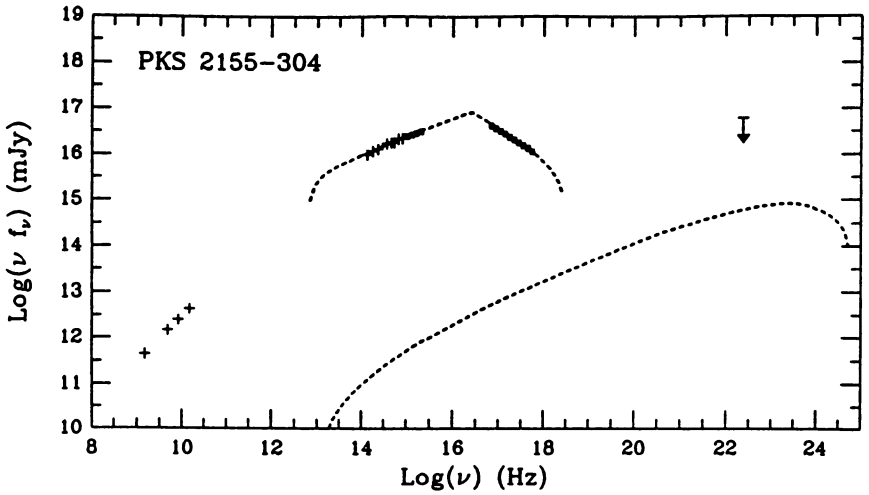

Fig. 2. The BBED as measured simultaneously on Nov. 13 1992. The arrow represents a generic EGRET upper limit. The dashed lines represent synchrotron and Inverse Compton emission from a relativistic jet described by the GMT model, with $\delta = 10$, $R_0 = 3\ 10^{13}$ cm, $R_{max} = 3\ 10^{16}$ cm, $B_0 = 3\ 10^3$ G, $B(R_{max}) = 150$ G.

size of the region and continuous acceleration is required.

Marscher et al. (1992) propose that the whole emission is produced by electrons accelerated at a shock at large distance from the nucleus allowing for lower energy densities and consequently longer cooling timescales, of the order of the observed variability timescales. In the case of PKS 2155–304 this implies a magnetic field of the order of ~ 0.25 G. The emission region has a sheet–like geometry determined by the radiative cooling length of particles accelerated in a shock front. X–rays would be closer to the front and the UV emission further "downstream". If the downstream region is on the observer side (reverse shock), the geometry is similar to the previous model. In the opposite case (direct shock) the Doppler effect would act so as to lengthen the observed lag, which would be a severe difficulty.

The tight limits on any observed spectral variability between the UV and X–ray bands could also pose a problem to the above models. In fact in both cases energy dependent variability implies spectral changes. However the ROSAT band is very close to the spectral break above which spectral variability is expected and the intensity amplitude of the observed variations is also small.

Specific computations are required to verify whether any of these models can quantitatively reproduce the observed light curves. As already mentioned the basic problem is to account for a large IR–UV emitting region and a short UV–X–ray time lag (and in fact both the models assume that the UV emitting region is larger

https://doi.org/10.1017/S0074180900175072 Published online by Cambridge University Press

than the X–ray one). It is important to stress that relativistic corrections depend not only on the velocity but also on the geometry of the emitting regions and on the origin/nature of the variations. For instance in the case of a propagating wave the simple Doppler correction for a time interval is $\propto \Gamma^2$. Therefore it is possible to ease the difficulty mentioned above if different relativistic corrections have to be applied to the variability and lag timescales.

5 The inverse Compton component: external vs. internal photons

Since blazars emit high frequency synchrotron radiation from regions of high photon density, it is inevitable that some γ–rays be produced by first order Compton scattering of the relativistic electrons off the synchrotron photons. This process is called "self-Compton" (SC). Using the inhomgeneous jet model by GMT, we were able to reproduce the observed BBED of the HPQ 3C 279 up to γ–ray energies (Maraschi, Ghisellini & Celotti 1992). We further applied the same model to the BL Lac object MKN 421 and to PKS 0537–441, which shows intermediate properties between the two classes (Maraschi, Ghisellini & Boccasile 1993). The required Γ's were between 5 and 7 and the radiation energy density was larger than the magnetic energy density, reflecting the ratio of SC and synchrotron luminosities.

It has been recently pointed out that the same relativistic electrons could also give rise to γ–rays by upscattering radiation external to the jet (EC). This could be due to photons coming directly from the accretion disk (Dermer, Schlickeiser & Mastichiadis, 1992), or by these very photons after isotropization by scattering in surrounding material, or by photons directly emitted by the broad line region (Sikora, Begelman & Rees, 1993). The latter two components (to which we will refer cumulatively as BLR), being isotropic within a region of radius R_{blr}, are seen enhanced in the comoving frame, due to relativistic aberration and blueshift, while the first is severely dimmed except for small distances from the disk. In the comoving frame, the ratio between the energy density of external BLR radiation U_{blr} and the magnetic energy density U_B is (omitting factors of order unity)

$$\frac{U_{blr}}{U_B} \sim \frac{L_{45}}{B^2}\,\frac{a}{0.1}\left(\frac{\Gamma}{10}\right)^2\left(\frac{10^{18}\mathrm{cm}}{R_{blr}}\right)^2 \qquad (1)$$

where a is the luminosity fraction scattered or emitted in the BLR, $R_{blr} > R_\gamma$, and R_γ is the location of the γ–ray emitting region. Assuming that the energy density of synchrotron photons U_S is comparable to U_B, eq. (1) shows that U_{blr} can be dominant provided that: 1) Γ is relatively large; 2) the 'BLR' exists; 3) the γ–ray emitting region is inside the 'BLR'.

In Ghisellini & Maraschi (1993) we have reconsidered the cases of 3C 279, PKS 0537–441 and MKN 421, suggesting that the EC process may contribute significantly to the observed γ–rays in the first two cases, but probably not in MKN 421 and other BL Lacs with *intrinsically* weak lines.

In general, the relative luminosities of the three processes, synchrotron (SY), Self Compton (SC), and inverse Compton off external photons (EC), are determined by the relative values of the energy densities U_B, U_S and U_{blr}:

$$L_S \propto NU_B; \qquad L_{SC} \propto NU_S; \qquad L_{EC} \propto NU_{blr} \tag{2}$$

where N is the total number of relativistic particles, and $U_S \propto L_S$.

A first criterion to distinguish observationally between the SC and EC mechanisms is based on the spectral shape of the two components. In fact the SC spectrum is fixed if the SY spectrum is known. Since the external photons are expected to have a narrower spectrum and a higher average energy than the SY ones, for a given SY spectrum, L_{EC} is more peaked toward the highest energies, while L_{SC} is broader. However, due to the wide bands where observations are lacking (FIR, hard X–ray soft γ–ray), a purely spectral discrimination though possible in principle seems hard in the near future.

Variability may be a more powerful test of SC or EC models. In fact we know that γ–rays are strongly and rapidly variable. 3C 279 was found to vary by a factor two in few days and by larger factors over few months (Kniffen et al. 1993). External radiation is not expected to vary by large factors on these time scales. The first prediction of both Compton models is that L_S and L_{SC} or L_{EC} should vary in a correlated fashion.

From eq. (2) we see that if variations are due to N, $\Delta L_{EC} \propto \Delta L_S$, while $\Delta L_{SC} \propto \Delta L_S^2$. Thus by measuring the variability in the ranges close to the maximum power output we can hope to test Compton models and distinguish between different sources of soft photons.

A less naive approach may consider a feed back of the large energy losses on the particle distribution function. In fact the estimated cooling times are short in most cases. Assuming that relativistic particles are continuously injected in the emitting region, the distribution function can be derived by means of a continuity equation. If the injected power is P_i, the steady particle density N (at energies where cooling dominates over escape and adiabatic losses) is

$$N \propto \frac{P_i}{U_B + U_S + U_{blr}} \tag{3}$$

Note that, for the energies we are interested in, only the first order scattering is important, the second order being cut off by the Klein Nishina regime. This is taken into account approximately by neglecting U_{SC} and U_{EC} in eq. (3).

Assume for the moment that U_{blr} is negligible. For sufficiently small P_i, we will have $U_B > U_S$, so that synchrotron radiation dominates the radiation losses. Combining eq. (2) with eq. (3) one can easily find that $L_S \propto P_i$ and therefore $L_{SC} \propto P_i^2$. Viceversa, at sufficiently large P_i, we will have $U_B < U_S$. In this case SC dominates the bolometric output, so that $L_{SC} \propto P_i$ and $L_S \propto P_i^{1/2}$.

https://doi.org/10.1017/S0074180900175072 Published online by Cambridge University Press

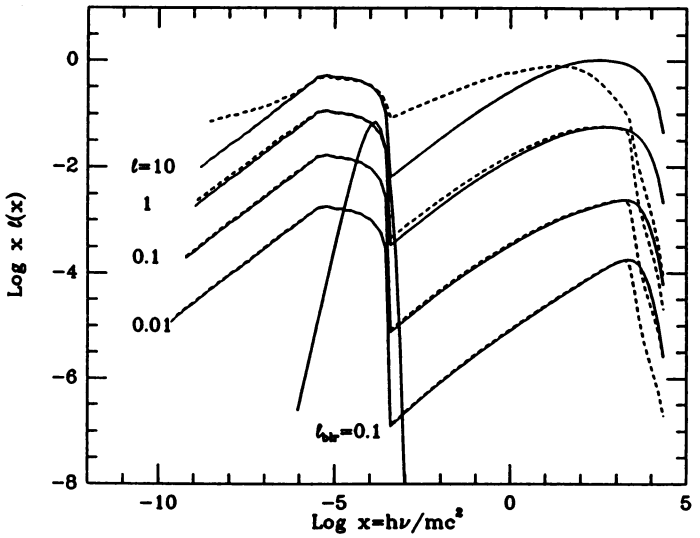

Fig. 3. *Continuous lines:* "Self-consistent" Synchrotron and inverse Compton emission spectra from relativistic electrons injected with given compactness ℓ into a region with $B = 10\ G$, $R = 3\ 10^{16}$ cm. Electrons cool by SY, Self Compton (SC) and External Compton (EC) on UV photons of compactness $\ell_{blr} = 0.1$ (shown in the fig. as the narrow peaked distribution). For small injected ℓ, the main cooling procees is EC so that the high energy spectrum reflects the electron spectrum. For large ℓ, the high energy radiation is mainly produced by the SC mechanism, resulting in a smoother high energy spectrum. *Dashed lines:* Same cases, but including pair production and radiation by the created pairs. The highest energy photons are absorbed by photon–photon collisions even for very small ℓ, due to the presence of the UV photon distribution. For $\ell > 10$ pair effects modify the entire spectrum. Note that the SY luminosity $\propto \ell$ for small compactnesses, and becomes $\propto \ell^{1/2}$ for large ℓ.

Let us now consider U_{blr}. Since it does not depend on P_i, we have for L_{EC} the same behaviour as L_S.

Hence, in all cases, when changing the injected power in relativistic electrons the SC luminosity should change more than the S one, while the EC and S emission should change by the same amount.

Therefore we have a simple and potentially powerful way of checking if the origin of the γ–rays in blazars are due to SC or EC radiation. Of course this is simple in theory, but it may prove difficult in reality, because:

i) the comparison discussed above refers to the entire (frequency integrated) S, SC and EC luminosities, while we observe in restricted energy bands;

ii) the emission region may not be homogeneous, with multiple components;

iii) we have assumed a constant bulk Lorentz factor and a constant energy density for the external radiation. If Γ changes, instead of P_i, then U_{blr} changes also, possibly inducing a variation of the γ–ray emission larger than the synchrotron one even when the external radiation is dominant. In this respect estimates of Γ

https://doi.org/10.1017/S0074180900175072 Published online by Cambridge University Press

at different epochs, from the superluminal motion, are extremely valuable.

To illustrate the above points we have computed SY, SC and EC spectra with the following assumptions: relativistic electrons are injected continuously in a source of radius $R = 3\ 10^{16} cm$, $B = 10\ G$, with spectrum $Q(\gamma) \propto \gamma^{-2}$ between $\gamma_{min} = 3 \times 10^3$ and $\gamma_{max} = 3 \times 10^4$. The injected power corresponds to an injected compactness ℓ, while the external radiation energy density (as seen in the comoving frame) corresponds to $\ell_{blr} = 0.1$. The spectra are computed with an iterative method, which allows the effects of photon–photon absorption and pair cascades to be taken into account. The computed spectra are shown in Fig. 3 for varying ℓ and fixed B and ℓ_{blr}.

6 Conclusions

The BBED of blazars can be decomposed in two smooth broad components, the first extending from the radio to the UV and in some cases X–ray spectral regions, the second from the X–ray up to the γ–ray bands. The relation between the two is a strong constraint for theoretical models in which the first component is interpreted as synchrotron and the second as Compton emission from the same relativistic electrons. A complete and simultaneous coverage of this enormous frequency range is desirable, but not easy to obtain in the short term. However, a very important quantity for an understanding of the physics of the emission region, is the luminosity ratio of the two components. Thus simultaneous observations in frequency bands close to the peaks in the power per decade, i.e. IR–opt–UV and γ–ray observations are essential.

Depending on the soft photons available for upscattering (either synchrotron photons or photons external to the jet), the relation between the low frequency and high frequency spectrum is expected to be different, with regard to both spectral shape and correlated variability. More theoretical work is needed in the area of time dependent models to explore a range of possibilities.

The long life–time expected for the Compton Gamma Ray Observatory gives us a tremendous opportunity to carry out systematic studies of correlated variability which may give us direct insight on the energy input and radiation losses of high energy particles in relativistic jets.

7 References

Bertsch, D.L. et al., 1993, ApJ, 405, L21

Blandford, R.D. & Rees, M.J., 1978, in "Pittsburgh Conference on BL Lac Objects", ed. A.N. Wolfe (Pittsburgh University Press), p. 328

Bregman, J.N., 1985, ApJ, 288, 32

Celotti, A., Maraschi, L. & Treves, A., 1991, ApJ, 337, 403

Dermer, C.D., Schlickeiser, R. & Mastichiadis, A., 1992, AA, 256, L27

Ghisellini, G., 1993, proc. of the Cospar Symposium (Washington), in press.

Ghisellini, G. & Maraschi, L., 1989, ApJ 340, 181
Ghisellini, G. & Maraschi, L., 1993, Proc. 2nd Compton Symp., Maryland, in press
Ghisellini, G., Maraschi, L. & Treves, A., 1985, A.A., 146, 204 (GMT)
Ghisellini, G., Maraschi, L., Tanzi, E. & Treves, A., 1986, ApJ, 310, 317
Ghisellini, G., Padovani, P., Celotti, A. & Maraschi, L., 1993, ApJ, 407, 65
Hartmann, R.C. et al. 1993, Proc. 2nd Compton Symp., Maryland, in press.
Hartman, R.C. et al., 1992, ApJ, 385, L1.
Hunter, S.D. et al., 1993a, ApJ, 409, 134.
Hunter, S.D. et al., 1993b, AA, 272, 59
Impey, C.D. & Neugebauer, G., 1988, AJ, 95, 307
Kniffen, D.A. et al. 1993, ApJ, 411, 133
Königl, A., 1989, in "BL Lac Objects", eds. L. Maraschi, T. Maccacaro and M–H. Ulrich (Springer–Verlag), p. 321
Kühr, H., Witzel, A., Pauliny–Toth, I.I.K & Nauber, U., 1981, AA (Suppl), 45, 367.
Landau, R. et al., 1986, ApJ, 308, 78
Lin, Y.C., et al., 1992, ApJ, 401, L61
Madau, P., Ghisellini, G. & Persic, M., 1987, MNRAS, 224, 257
Mannheim, K., 1993, AA, 269, 67
Maraschi, L., Ghisellini, G. & Boccasile, A. 1993, Proc. Physics of AGNs, Cambrige, in press
Maraschi, L., Ghisellini, G. & Celotti, A. 1992, ApJ, 397, L5
Maraschi, L., Ghisellini, G., Tanzi, E.G., & Treves, A., 1986, ApJ, 310, 325.
Marscher, A.P., Gear, W.K. & Travis, J.P. 1992, in "Variability of blazars", eds. E. Valtaoja and M. Valtonen (Cambridge Univ. Press), p. 85
Marscher, A.P., 1993, in Astrophys. Jets, eds. Burgarella, D., Livio, M. & O'Dea C., Cambridge University Press, in press.
Pian, E. & Treves, A., 1993, ApJ, 416, 130
Punch, M. et al., 1992, Nature, 358, 477
Sambruna, et al., 1993, ApJ, submitted.
Sikora, M., Begelman, M.C. & Rees, M.J., 1993, ApJ, in press
Sikora, M., 1993, ApJ Suppl. in press (proceed. of the 142 IAU Symp.)
Tanzi, E. et al., 1989, in BL Lac Objects, Lecture Notes in Physics, 334, p.171, eds. Maraschi, L., Maccacaro, T. & Ulrich M.H., Springler–Verlag
Thompson, D.J., et al., 1993a, ApJ, 410, 87
Thompson, D.J., et al., 1993b, ApJ, 415, L13
Treves, A. et al., 1993, ApJ, 406, 447
Valtoja, E., Lahteenmaki A. & Terasranta H., 1992, preprint
Wall, J.V., & Peacock, J.A., 1985, MNRAS, 216, 173.
Wiren S., Valtoja E., Terasranta H. & Kotilainen, 1992, preprint
Worral, D.M. & Wilkes, B.J., 1990, ApJ, 360, 396